Molecular Cancer

RESEARCH

Open Access

EIF4E-mediated biogenesis of circPHF14 promotes the growth and metastasis of pancreatic ductal adenocarcinoma via Wnt/β-catenin pathway

Zhou Fang[1†], Zhuo Wu[1†], Chao Yu[1†], Qingyu Xie[1†], Liangtang Zeng[1] and Rufu Chen[1*]

Abstract

Background CircRNAs are critically involved in the development and progression of various cancers. However, their functions and mechanisms in pancreatic ductal adenocarcinoma (PDAC) remain largely unknown.

Methods CircPHF14 (hsa_circ_0079440) was identified through the analysis of RNA sequencing data from PDAC and normal adjacent tissues. The biological functions of circPHF14 were then evaluated using CCK8, EdU, transwell, colony formation, wound healing assays, as well as pancreatic orthotopic xenograft and liver metastasis models. The interaction mechanisms between circPHF14 and PABPC1, which enhance the stability of WNT7A mRNA, were investigated through RNA pull-down, mass spectrometry, RNA Immunoprecipitation (RIP), and actinomycin D assays. The role of EIF4E in promoting circPHF14 biogenesis was examined using RIP, and western blotting.

Results In this study, we observed a significant upregulation of circPHF14 in both clinical PDAC samples and cell lines. Functionally, circPHF14 enhanced PDAC proliferation and metastasis both in vitro and in vivo. Mechanistically, circPHF14 interacted with PABPC1 to stabilize WNT7A mRNA, thereby activating the Wnt/β-catenin pathway, which subsequently upregulated SNAI2 and initiated Epithelial-Mesenchymal Transition (EMT) in PDAC. Additionally, EIF4E was found to bind PHF14 pre-mRNA, facilitating circPHF14 biogenesis. Finally, we developed a lipid nanoparticle (LNP) formulation encapsulating sh-circPHF14 plasmids and confirmed its anti-tumor efficacy in a patient-derived xenograft (PDX) model.

Conclusion EIF4E-mediated biogenesis of circPHF14 stabilizes WNT7A mRNA via interaction with PABPC1, which subsequently activates the Wnt/β-catenin pathway, promoting the growth and metastasis of PDAC. These findings indicate that circPHF14 holds promise as a biomarker and therapeutic target for PDAC.

Keywords Pancreatic ductal adenocarcinoma, circPHF14, WNT7A, PABPC1, EIF4E, LNP

[†]Zhou Fang, Zhuo Wu, Chao Yu and Qingyu Xie contributed equally to this work.

*Correspondence:
Rufu Chen
sychenrufu@scut.edu.cn

[1]Department of Pancreatic Surgery, Department of General Surgery, Guangdong Provincial People's Hospital, Guangdong Academy of Medical Sciences, Southern Medical University, Guangzhou, Guangdong Province, China

Introduction

Pancreatic ductal adenocarcinoma (PDAC) is a highly aggressive malignancy that accounts for over 90% of pancreatic cancer cases [1]. Its biological characteristics contribute to its invasive nature, including early infiltration of adjacent tissues, local lymph node metastasis, and distant metastasis. With a 5-year survival rate of only 11%, PDAC is projected to become the second leading cause of cancer-related deaths by 2030 [2, 3]. Most PDAC patients are diagnosed at advanced stages, missing the window for curative surgery. Even for those eligible for surgery, long-term survival remains elusive [4]. Chemoradiotherapy and immunotherapy have limited efficacy in patients with unresectable PDAC [5]. Therefore, it is crucial to elucidate the molecular mechanisms underlying PDAC development, identify effective biomarkers, and develop novel molecular targets for its treatment.

Circular RNAs (circRNAs) are a class of endogenous non-coding RNAs. Unlike traditional linear RNAs, circRNAs lack both the 5' cap and 3' poly(A) tail, making them more stable and less prone to degradation [6]. These intrinsic properties make circRNAs more suitable as effective cancer biomarkers and novel therapeutic targets [7, 8]. In recent years, studies have increasingly shown that circRNAs play extensive regulatory roles in PDAC, especially in its initiation, progression, and metastasis [9]. For example, our previous research demonstrated that circBFAR promotes PDAC progression via the miR-34b-5p/MET/Akt axis [10]. However, most previous studies have focused primarily on circRNAs' role as miRNA sponges. In fact, circRNAs perform various biological functions, including interacting with proteins, regulating transcription and splicing, or translating short peptides [7]. Recent studies suggest that aberrant regulation of circRNA biogenesis significantly influences downstream signaling pathways, contributing to the onset and progression of various cancers [11]. For example, ZEB1 persistently promotes the biogenesis of circNIPBL, thereby enhancing bladder cancer metastasis [12]. The biogenesis of circRNAs is primarily mediated through selective back-splicing of precursor mRNAs [13]. Specific RNA-binding proteins (RBPs), such as QKI and FUS, can bind to defined regions of precursor mRNAs to facilitate circRNA formation [14, 15]. Nevertheless, the mechanistic role of circRNAs and their biogenesis in the development and progression of PDAC remains poorly understood and warrants further investigation.

The Wnt signaling pathway is a classical signal transduction cascade that plays a crucial regulatory role in cancer progression [16]. WNT7A, a ligand of the Frizzled family of seven-transmembrane receptors, primarily mediates biological processes such as cell proliferation, differentiation, and migration by activating the canonical Wnt pathway [17]. Additionally, Wnt signaling regulates β-catenin stability, which activates Epithelial-Mesenchymal Transition (EMT)-related transcription factors such as SNAIL, SNAI2, and TWIST [18, 19]. These transcription factors suppress the expression of the key epithelial marker E-cadherin, resulting in reduced cell-cell adhesion and promoting a more migratory and invasive mesenchymal phenotype, which drives the progression and metastasis of various advanced cancers and is closely linked to poor prognosis [20]. Previous studies have shown that inhibiting WNT7A expression significantly suppresses tumor progression and distant metastasis in vivo [21]. Therefore, investigating the molecular mechanisms of sustained activation of the WNT7A-mediated Wnt/β-catenin signaling pathway and its key regulatory molecules may provide potential therapeutic targets for PDAC.

Nanomedicine has recently emerged as a promising strategy for cancer treatment. Nanoparticles exhibit high stability, encapsulate and deliver DNA, siRNA, mRNA, and small-molecule drugs, and possess excellent targeting capabilities [22, 23]. To explore the clinical potential of circRNAs in PDAC treatment, we developed a lipid nanoparticle (LNP) system that effectively regulates circRNAs expression in tumors, exerting anti-tumor effects.

In this study, we discovered that circular RNA circPHF14 (hsa_circ_0079440) is significantly upregulated in PDAC and closely correlates with poor patient prognosis. Functional analyses revealed that circPHF14 overexpression significantly enhances the migration and proliferation of PDAC cells in both in vitro and in vivo models. Mechanistically, circPHF14 recruits the PABPC1 protein to the 3' untranslated region (3'-UTR) of WNT7A mRNA, stabilizing WNT7A mRNA and further activating the WNT7A/β-catenin signaling pathway. Additionally, circPHF14 upregulates SNAI2 expression through the Wnt pathway, promoting EMT. We also found that EIF4E is another key molecule upregulated in PDAC tissues. EIF4E binds to intron 13 (125–176 nt) and intron 16 (32,726–32,777 nt) of PHF14 pre-mRNA, promoting back-splicing and accelerating circPHF14 formation. Building on these findings, we developed an LNP system encapsulating sh-circPHF14 plasmid, which demonstrated efficacy in inhibiting PDAC in patient-derived xenograft (PDX) models. These findings indicate that circPHF14 may serve as a promising therapeutic target for PDAC.

Materials and methods

Clinical samples

From October 2020 to October 2023, we collected pancreatic cancer tissue samples from 96 patients who underwent surgical treatment in the Department of

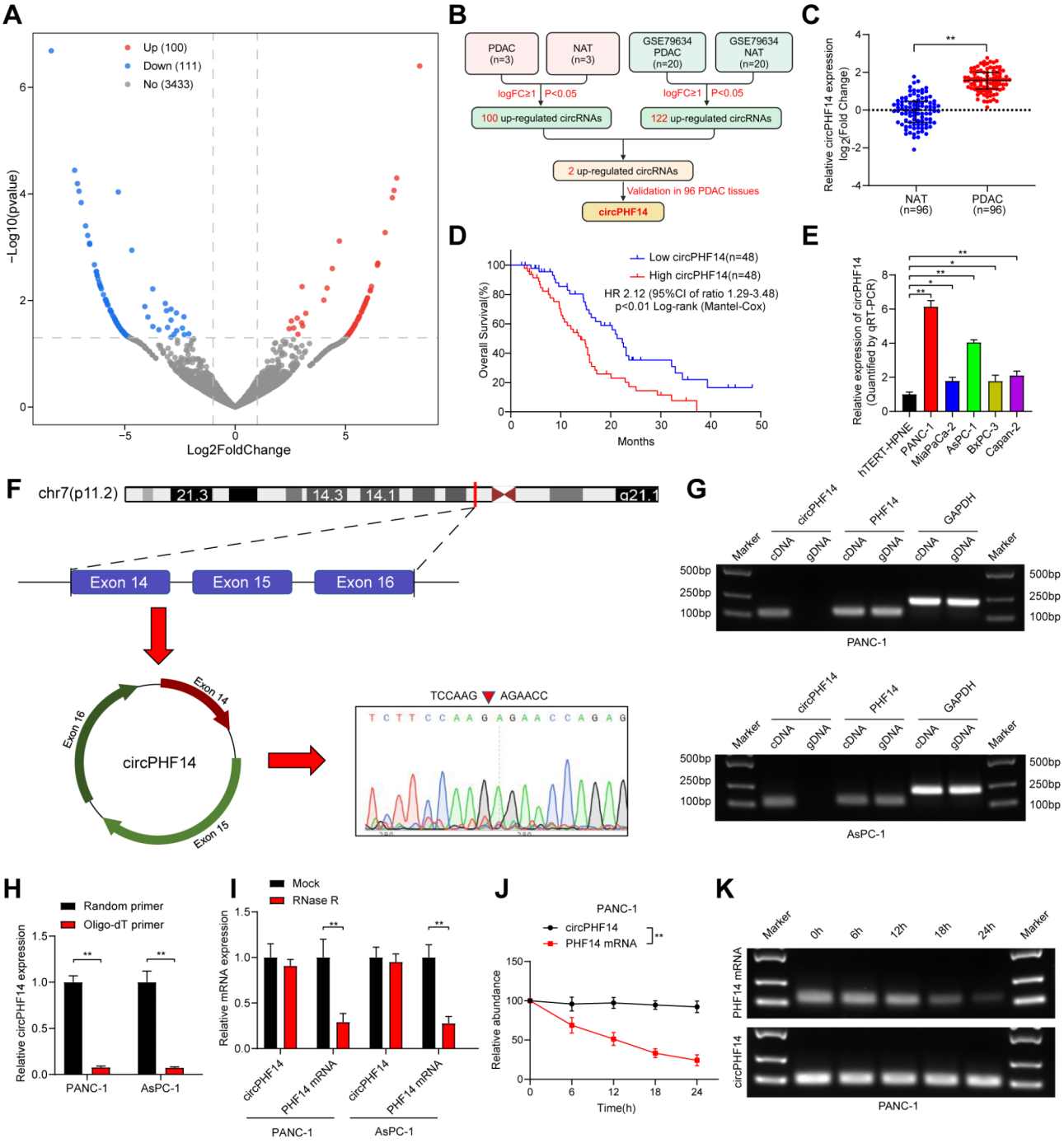

Fig. 1 Identification and characterization of circPHF14 in PDAC. (**A**) Volcano plot of differentially expressed circRNAs. (**B**) Schematic illustration of the screening process for upregulated circular RNAs in PDAC. (**C**) qRT-PCR analysis of circPHF14 expression in paired PDAC tissues ($n = 96$) and matched adjacent normal tissues (NATs, $n = 96$). (**D**) Kaplan-Meier analysis of OS in PDAC patients with low and high circPHF14 expressions. (**E**) Relative expression of circPHF14 across hTERT-HPNE, PANC-1, MiaPaCa-2, AsPC-1, BxPC-3, and Capan-2 cell lines, as measured by qRT-PCR. (**F**) Schematic representation of circPHF14 circularization and Sanger sequencing results at the splice junctions. (**G**) PCR analysis of circPHF14 and PHF14 in cDNA and gDNA from PANC-1 and AsPC-1 cells, with GAPDH as the loading control. (**H**) qRT-PCR analysis of circPHF14 expression using random primers and oligo-dT primers. (**I**) qRT-PCR analysis of circPHF14 and PHF14 mRNA expression in PANC-1 and AsPC-1 cells following RNase R treatment. (**J**, **K**) Stability assessment of circPHF14 and PHF14 mRNA in PANC-1 cells using actinomycin D assay (**J**) and agarose gel electrophoresis (**K**). Statistical analysis was performed using the Mann-Whitney U test in C and D, one-way ANOVA with Dunnett's test in E, and two-tailed Student's t-test in H, I, and J. Error bars represent the standard deviation from three independent experiments. *$p < 0.05$, **$p < 0.01$

Pancreatic Surgery at Guangdong Provincial People's Hospital in Guangzhou, China. Clinical data were obtained from medical records, and follow-up information was gathered through telephone consultations or death certificates. This experimental protocol was approved by the Ethics Review Committee of Guangdong Provincial People's Hospital (Ethics No.: KY2024-528), and all patients signed informed consent forms.

Western blot

Cells were lysed using Radioimmunoprecipitation Assay (RIPA) lysis buffer (CWBIO, China) supplemented with 1% protease inhibitor and 1% phosphatase inhibitor. After centrifugation at 12,000 rpm for 30 min at 4 °C, the supernatant was collected, and protein concentration was determined using a Bicinchoninic Acid (BCA) protein assay kit (CWBIO, China). Proteins were separated using SDS-PAGE (Epizyme, China) and transferred onto PVDF membranes (MERCK, Germany). Membranes were blocked with rapid protein-free blocking solution (Epizyme, China) and incubated overnight with primary antibodies at 4 °C. After three washes with Tris-Buffered Saline with Tween-20 (TBST), membranes were incubated with secondary antibodies at room temperature for 1 h. Following three more washes with TBST, protein levels were detected using an ultrasensitive ECL chemiluminescence substrate (Tanon, China). Antibodies are listed in Table S3.

RNA pull-down assay

An RNA pull-down assay was conducted to identify circPHF14-binding proteins in PDAC cells. Biotinylated circPHF14 and NC probes were incubated with PDAC cell lysates overnight at 4 °C. The next day, the lysates were incubated with magnetic beads (Thermo Scientific, USA) at 4 °C for 3 h. Proteins bound to circPHF14 were eluted, stained using the Pierce Silver Stain Kit (Thermo Scientific, USA), and differential bands were analyzed via mass spectrometry.

RNA immunoprecipitation (RIP) assay

The RIP assay was performed using an RNA immunoprecipitation kit (BersinBio, China) following the manufacturer's instructions. Briefly, 2×10^7 PDAC cells were lysed using RIP lysis buffer. Anti-IgG, anti-AGO2, anti-PABPC1, or anti-EIF4E antibodies were incubated with the cell lysate at 4 °C overnight. The following day, magnetic beads were added to the antibody-lysate complexes and incubated at 4 °C for 3 h. RNA samples were then precipitated, reverse-transcribed into cDNA, and analyzed by Quantitative Real-Time Polymerase Chain Reaction (qRT-PCR).

The supplementary materials provide additional information on the materials and methods employed.

Results

Identification of circPHF14 and circPHF14 is upregulated in PDAC

To identify key circRNAs involved in the proliferation and metastasis of PDAC, we conducted high-throughput sequencing on PDAC specimens and paired normal adjacent tissues (NATs) from three patients (Fig. 1A). Next, we cross-referenced our sequencing data (GSE289888) with publicly available circRNA data from the GEO database (GSE79634) and identified two circRNAs that were upregulated in PDAC tissues compared to NATs ($\log FC \geq 1$ and $p < 0.05$) (Fig. 1B). We subsequently evaluated the circRNAs identified from the screening in a cohort of 96 PDAC patients and found that circPHF14

Table 1 Association between circPHF14 expression levels and clinicopathologic characteristics of PDAC patients

Characteristics	No. of cases	circPHF14 expression level		
		Low	High	*p*-value[a]
Total cases	96	48	48	
Gender				0.682
Male	52	27	25	
Female	44	21	23	
Age				0.092
≤ 60	36	14	22	
> 60	60	34	26	
Differentiation				0.570
Poor	4	3	1	
Moderate	32	15	17	
Well	60	30	30	
TNM stage				**0.008****
Stage I	47	31	16	
Stage II	38	14	24	
Stage III	11	3	8	

Abbreviations: No. of cases = number of cases. [a]Chi-square test, *$p < 0.05$, **$p < 0.01$

(hsa_circ_0079440) was significantly overexpressed in PDAC tissues (Fig. 1C). Kaplan-Meier survival analysis indicated that high circPHF14 expression correlated with shorter overall survival (OS) in PDAC patients (Fig. 1D). Additionally, Cox univariate and multivariate analyses identified circPHF14 expression as an independent predictor of poor prognosis (Table 1, S1). These findings suggest a potential role for circPHF14 in PDAC development and progression.

We assessed circPHF14 expression in five human pancreatic cancer cell lines (PANC-1, MiaPaCa-2, AsPC-1, BxPC-3, and Capan-2) and one human normal pancreatic ductal epithelial cell line (hTERT-HPNE). CircPHF14 was found to be upregulated to varying degrees across all pancreatic cancer cell lines. The two cell lines with the highest expression levels, PANC-1 and AsPC-1, were selected for further investigation (Fig. 1E). To confirm the circular structure of circPHF14, we performed Sanger sequencing on qRT-PCR products amplified using circPHF14-specific primers, which verified its back-splicing junction (Fig. 1F). PCR analysis of complementary DNA (cDNA) and genomic DNA (gDNA) demonstrated that PHF14 was present in both cDNA and gDNA, whereas circPHF14 was only detected in cDNA, indicating its formation via back-splicing rather than genomic rearrangement (Fig. 1G). Furthermore, reverse transcription using random primers revealed higher circPHF14 expression compared to oligo-dT primers, suggesting that circPHF14 has fewer poly-A tails (Fig. 1H). After RNase R and actinomycin D treatments, circPHF14 showed greater stability than linear PHF14 (Fig. 1I-1 and Fig. S1A, B). Collectively, these results confirm that circPHF14 is a stable, covalently closed circular RNA derived from exons 14–16 of the PHF14 gene.

CircPHF14 promotes PDAC proliferation and migration in vitro

To elucidate the biological function of circPHF14 in PDAC, we modulated circPHF14 expression in PANC-1 and AsPC-1 cells by transfecting them with small interfering RNA (siRNA) and circPHF14 overexpression plasmids. These approaches successfully achieved downregulation and overexpression of circPHF14 (Fig. 2A, 2 and Fig. S1C, D). We first assessed the effect of circPHF14 on cell proliferation using Cell Counting Kit-8 (CCK-8), 5-Ethynyl-2'-deoxyuridine (EdU), and colony formation assays. The results demonstrated that circPHF14 knockdown inhibited the proliferation of PANC-1 and AsPC-1 cells, whereas overexpression of circPHF14 had the opposite effect (Fig. 2C-2 and Fig. S1E-G). Additionally, transwell and wound healing assays revealed that circPHF14 knockdown impaired cell migration, while overexpression of circPHF14 enhanced migration (Fig. 2F, 2 and Fig. S1H, I). Collectively, these findings indicate that circPHF14 overexpression enhances the proliferative and migratory capacity of PDAC cells.

CircPHF14 promotes tumorigenesis and development of PDAC in vivo

To investigate the in vivo effects of circPHF14 on PDAC, we injected PANC-1 cells stably transfected with sh-circPHF14 or the corresponding control sh-NC, as well as PANC-1 cells stably overexpressing circPHF14 or the corresponding control vector, into nude mice (Fig. 3A, 3). An orthotopic xenograft tumor model was established, and the results showed that tumors in the circPHF14 knockdown group were smaller and exhibited lower fluorescence intensity in In Vivo Imaging System (IVIS) images. In contrast, tumors derived from PANC-1 cells overexpressing circPHF14 displayed faster growth and higher fluorescence intensity compared to the control group (Fig. 3C, 3). Multiple immunohistochemical analyses revealed decreased levels of Ki-67 and N-cadherin, and increased E-cadherin levels in the circPHF14 knockdown group. Conversely, the circPHF14 overexpression group exhibited the opposite trend, indicating a correlation between circPHF14 expression and the levels of Ki-67, E-cadherin, and N-cadherin (Fig. 3E). These findings demonstrate that circPHF14 promotes tumorigenesis and progression of PDAC in vivo.

We developed a liver metastasis model to investigate the role of circPHF14 in promoting PDAC metastasis in vivo. The results demonstrated that mice injected with PANC-1 cells with circPHF14 knockdown exhibited a significant reduction in the number of liver metastatic nodules. Conversely, overexpression of circPHF14 in PANC-1 cells markedly enhanced the liver metastatic potential of PDAC (Fig. 3F, 3). These findings suggest that circPHF14 plays a critical role in promoting PDAC cell metastasis in vivo.

CircPHF14 regulates the Wnt/β-catenin signaling pathway in PDAC

To investigate the potential mechanism by which circPHF14 promotes PDAC proliferation and migration, we performed high-throughput RNA sequencing on PANC-1 cells overexpressing circPHF14 and their corresponding controls. The results indicated that 3,215 genes were upregulated in circPHF14-overexpressing PANC-1 cells ($\log FC \geq 1$, $p < 0.05$) (Fig. 4A). Kyoto Encyclopedia of Genes and Genomes (KEGG) pathway enrichment analysis suggested the activation of the Wnt signaling pathway (Fig. 4B). We then examined the expression profiles of key genes in this pathway. qRT-PCR analysis showed that WNT7A was significantly downregulated in circPHF14-knockdown PANC-1 cells and upregulated in circPHF14-overexpressing cells, suggesting that WNT7A is a downstream target of circPHF14 (Fig. 4C,

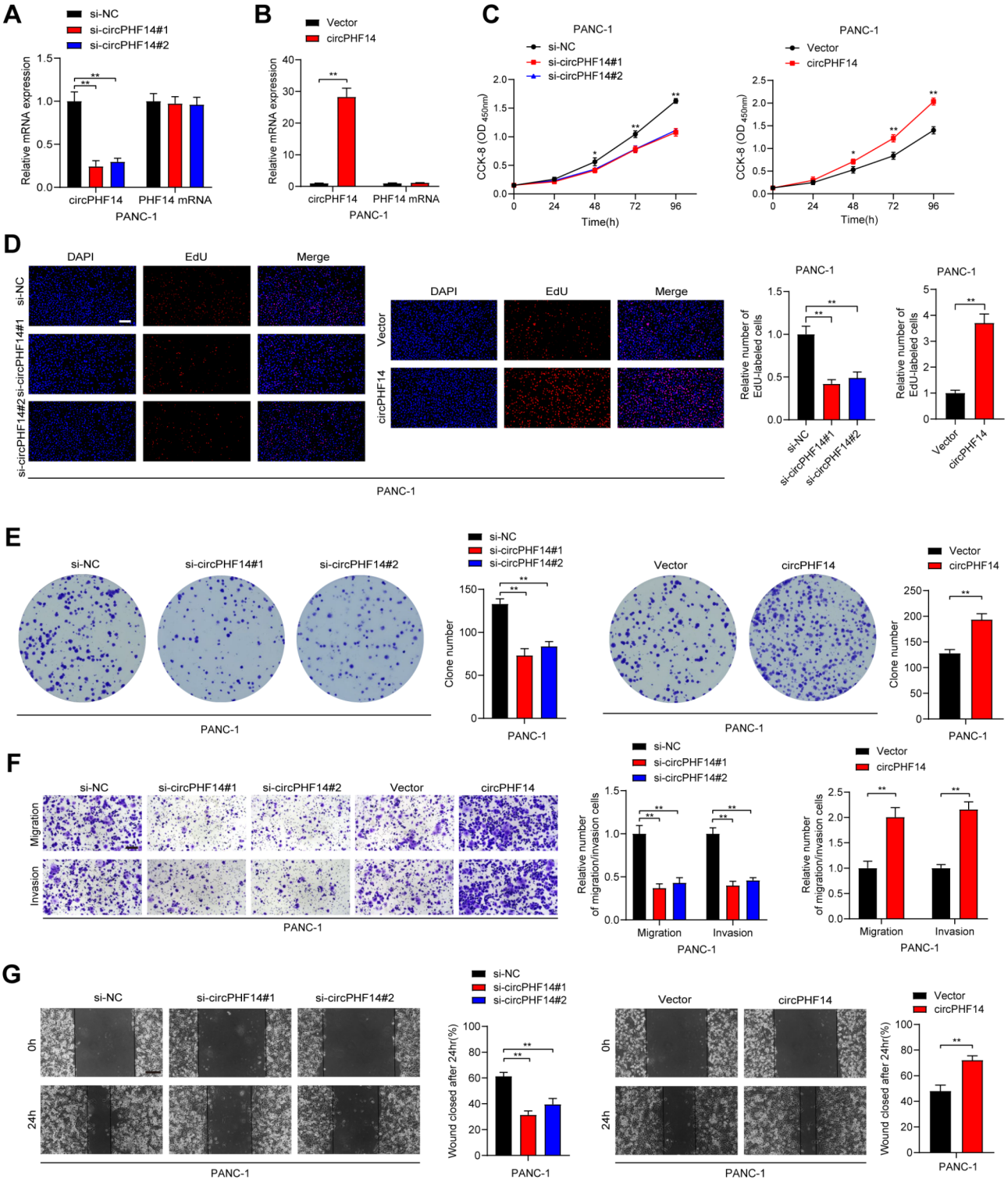

Fig. 2 (See legend on next page.)

(See figure on previous page.)

Fig. 2 CircPHF14 promotes proliferation, migration, and invasion of PANC-1 cells in vitro. (**A**, **B**) qRT-PCR analysis of circPHF14 and PHF14 expression levels in PANC-1 cells with circPHF14 knockdown (**A**), overexpression (**B**), and paired control cells. (**C**) Cell viability in PANC-1 cells after circPHF14 knockdown or overexpression, assessed using CCK-8 assay. (**D**) Representative images and quantification of EdU assays in PANC-1 cells following circPHF14 knockdown or overexpression, scale bar = 50 μm. (**E**) Representative images and quantification of colony formation assays in PANC-1 cells with circPHF14 knockdown or overexpression. (**F**) Representative images and quantification of Transwell migration and Matrigel invasion assays in PANC-1 cells with circPHF14 knockdown or overexpression, scale bar = 100 μm. (**G**) Representative images and quantitative analysis of wound healing assays in PANC-1 cells with circPHF14 knockdown or overexpression, scale bar = 100 μm. Statistical differences in **A**, **C**, **D**, **E**, **F**, and **G** were assessed using one-way ANOVA with Dunnett's test. The Two-tailed Student's t-test was used for **B**, **C**, **D**, **E**, **F**, and **G**. Error bars represent the standard deviation of three independent experiments. *$p < 0.05$, **$p < 0.01$

4). Previous studies have demonstrated that WNT7A mediates biological processes by activating the canonical Wnt pathway [17]. To confirm whether circPHF14 promotes PDAC proliferation and migration via the Wnt/β-catenin pathway, we modulated circPHF14 expression in PANC-1 and AsPC-1 cells and assessed the expression of core regulators in this pathway through Western blotting. The results showed that circPHF14 knockdown reduced WNT7A and β-catenin expression, while circPHF14 overexpression significantly increased their levels (Fig. 4E, 4).

We further investigated whether WNT7A, as a downstream target of circPHF14, promotes PDAC proliferation and metastasis. In vitro functional assays, including EdU, colony formation, Transwell, wound healing, and CCK-8 experiments, demonstrated that circPHF14 overexpression enhanced the proliferation and migration of PDAC cells, whereas WNT7A knockdown abolished these effects (Fig. 4G-4 and Fig. S2 A-E). We next investigated the critical role of circPHF14-mediated WNT7A in PDAC progression. A xenograft tumor model was successfully established using nude mice. Overexpression of circPHF14 significantly increased tumor volume and fluorescence intensity, as demonstrated by IVIS imaging results. In contrast, WNT7A knockdown markedly reversed the tumor-promoting effects of circPHF14 in vivo, emphasizing its significant contribution to tumor growth regulation (Fig. S2 F–H). To examine the metastatic characteristics of circPHF14-mediated WNT7A in PDAC in vivo, a liver metastasis model was constructed. The results indicated that WNT7A knockdown markedly reversed the metastasis-promoting effects of circPHF14, significantly reducing the number of liver metastatic nodules in mice (Fig. S2 I-K). Collectively, these findings demonstrate that circPHF14 promotes PDAC proliferation and metastasis by mediating WNT7A.

To further understand the significance of the Wnt/β-catenin pathway in circPHF14-mediated PDAC progression, we added the Wnt inhibitor XAV939 in vitro to block the pathway. Functional assays revealed that circPHF14 overexpression enhanced the proliferation and migration of PDAC cells, whereas XAV939 effectively abrogated these effects (Fig. 4L-4 and Fig. S3 A-D) These findings collectively demonstrate that circPHF14 promotes PDAC proliferation and migration by activating the Wnt/β-catenin pathway.

CircPHF14 exerts its function in PDAC cells through direct interaction with PABPC1

We investigated the mechanism by which circPHF14 upregulates WNT7A expression and activates the Wnt/β-catenin pathway. Given the importance of cellular localization for circRNA function, we first performed RNA nuclear-cytoplasmic fractionation and fluorescence in situ hybridization (FISH), revealing that circPHF14 is predominantly localized in the cytoplasm of PDAC cells (Fig. S4 A-D). Previous studies have suggested that cytoplasmic circRNAs primarily function by acting as molecular sponges or by interacting with RNA-binding proteins [6]. Initial RIP showed no significant enrichment of circPHF14 with AGO2 relative to IgG antibodies, suggesting that circPHF14 is unlikely to function as a miRNA sponge (Fig. S4 E). We then explored whether circPHF14 exerts its function through interactions with RNA-binding proteins.

To identify potential binding partners, we performed RNA pull-down assays using biotinylated probes targeting the back-splicing junction of circPHF14. Silver staining revealed a distinct band around 70 kDa in the biotinylated circPHF14 probe group, which was identified as PABPC1 via mass spectrometry (Fig. 5A, 5 and Fig. S4 F). Subsequent Western blot analysis of RNA pull-down samples confirmed that circPHF14 significantly enriched PABPC1 (Fig. 5C, 5). Similarly, RIP assays using anti-PABPC1 antibodies showed that circPHF14 was significantly enriched compared to the IgG control (Fig. 5E and Fig. S4 G). Furthermore, FISH and immunofluorescence analyses demonstrated co-localization of circPHF14 and PABPC1 in the cytoplasm of PDAC cells (Fig. 5F).

To further identify the PABPC1 binding site on circPHF14, we conducted consecutive deletion assays using truncated circPHF14 sequences. The results indicated that PABPC1 was enriched in the 201–291 nt region of circPHF14 (Fig. 5G, 5). Additionally, predictions from catRAPID (http://service.tartaglialab.com/page/catrapid_group) suggested that the 216–267 nt segment is the potential binding site of PABPC1 on circPHF14 (Fig. S4 H) [24]. RIP assays confirmed that mutation of the

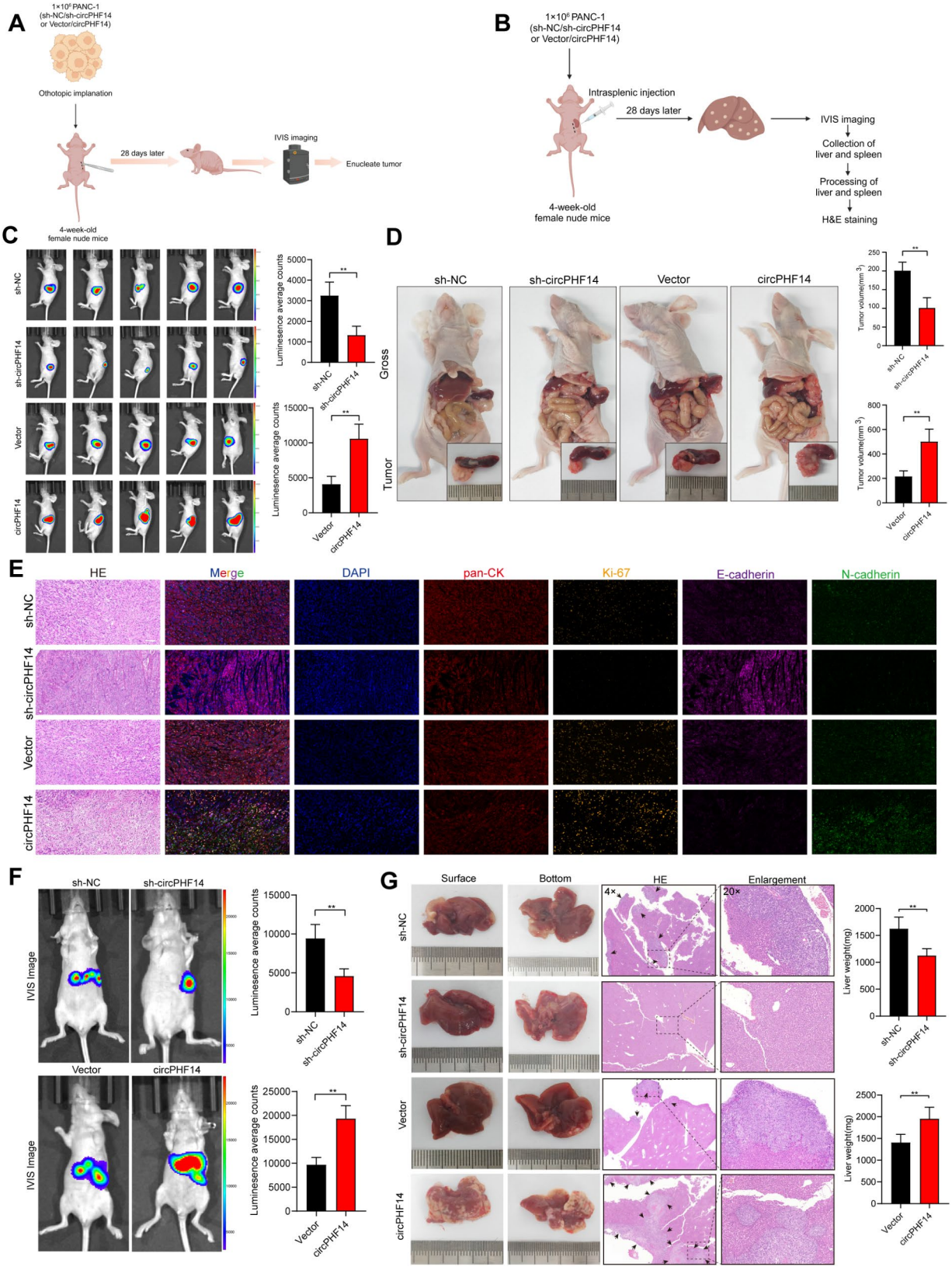

Fig. 3 (See legend on next page.)

(See figure on previous page.)

Fig. 3 CircPHF14 promotes PDAC growth and metastasis In vivo. (**A**, **B**) Schematic representation of the xenograft tumor model in nude mice. (**C**, **D**) IVIS images (**C**) and harvested pancreatic tumors (**D**) from the orthotopic xenograft tumor model, along with statistical analysis ($n = 5$ mice per group). (**E**) Representative images of multiplex immunohistochemical staining for pan-CK, Ki-67, E-cadherin, and N-cadherin in the orthotopic xenograft tumor model. Scale bar = 100 μm. (**F**, **G**) IVIS images (**F**) and harvested liver metastases with HE staining (**G**) from the liver metastasis model, along with statistical analysis ($n = 5$ mice per group). Statistical analysis in **C**, **D**, **F**, and **G** was performed using a two-tailed Student's t-test. Error bars represent the standard deviation from three independent experiments. $^{*}p < 0.05$, $^{**}p < 0.01$

216–267 nt region of circPHF14 significantly reduced its enrichment with PABPC1 (Fig. 5I). Additionally, an RNA pull-down assay using a biotin-labeled probe targeting the circPHF14 216–267 nt mutant revealed that this mutation abolished the ability of circPHF14 to enrich PABPC1 (Fig. 5J and Fig. S4 I). These findings indicate that the 216–267 nt sequence of circPHF14 is essential for its interaction with PABPC1.

To further investigate the functional role of PABPC1 in circPHF14-mediated promotion of cell proliferation and migration, we conducted in vitro assays. The results demonstrated that PABPC1 knockdown reversed the circPHF14 overexpression-induced enhancement of cell proliferation and migration (Fig. S4 J-N). Moreover, compared to wild-type circPHF14, the circPHF14 mutant (Δ216–267 nt), which cannot bind PABPC1, exhibited no significant effect on cell proliferation or migration (Fig. S5 A-E). Collectively, these results suggest that circPHF14 promotes PDAC cell proliferation and migration by directly interacting with PABPC1.

CircPHF14/PABPC1 complex promotes WNT7A mRNA stability

Previous studies have shown that circRNAs can regulate the expression of their associated RBPs [25]. However, western blot analysis confirmed that circPHF14 does not influence PABPC1 protein levels (Fig. S6 A-D). Given that WNT7A is a downstream target of circPHF14, we investigated whether PABPC1 cooperates with circPHF14 to regulate WNT7A expression. qRT-PCR and western blot analyses revealed that PABPC1 knockdown significantly reversed the upregulation of WNT7A induced by circPHF14 overexpression (Fig. 5K and Fig. S6 E). Furthermore, the mutant circPHF14 (Δ216–267 nt), which cannot bind PABPC1, showed no significant effect on WNT7A expression compared to the wild-type circPHF14 (Fig. 5L and Fig. S6 F). These findings suggest that circPHF14 regulates WNT7A expression by forming a complex with PABPC1. Previous studies have also indicated that PABPC1 can regulate mRNA stability by binding to the 3'-UTR of target mRNAs [26, 27]. We further predicted the interaction between PABPC1 and the 3'-UTR of WNT7A mRNA using the RPISeq website (http://pridb.gdcb.iastate.edu/RPISeq/) [28]. Scores from both the RF and SVM classifiers were greater than 0.5, indicating a high likelihood of interaction between PABPC1 and the 3'-UTR of WNT7A mRNA (Fig. S6 G).

To further confirm the interaction between PABPC1 and the 3'-UTR of WNT7A mRNA, a dual-luciferase assay was performed. Overexpression of circPHF14 significantly enhanced luciferase activity associated with the WNT7A mRNA 3'-UTR, an effect that was reversed by PABPC1 knockdown (Fig. 5M and Fig. S6 H). In contrast, the mutant circPHF14 (Δ216–267 nt) had no significant effect on luciferase activity linked to the WNT7A mRNA 3'-UTR (Fig. 5N and Fig. S6 I). These results support the hypothesis that the circPHF14/PABPC1 complex regulates WNT7A expression via the WNT7A mRNA 3'-UTR.

Next, we examined the effect of circPHF14 on WNT7A mRNA stability using actinomycin D assays. The results revealed that circPHF14 downregulation significantly shortened the half-life of WNT7A mRNA (Fig. 5O, 5 and Fig. S6 J, K). Conversely, overexpression of circPHF14 extended the half-life of WNT7A mRNA, an effect that was reversed by PABPC1 knockdown (Fig. 5Q, 5 and Fig. S6 L, M). The mutant circPHF14 (Δ216–267 nt) similarly exhibited no significant effect on the stability of WNT7A mRNA (Fig. 5S, 5 and Fig. S6N, O). Moreover, PABPC1 overexpression extended the half-life of WNT7A mRNA, which was reversed by circPHF14 knockdown (Fig. 5U, 5 and Fig. S3 P, Q). These findings indicate that circPHF14 stabilizes WNT7A mRNA in PDAC cells by forming a complex with PABPC1 and targeting the 3'-UTR of WNT7A mRNA.

Previous studies have highlighted the importance of direct interactions between specific sequences of the 3'-UTR enriched with adenosine and uridine (AU)-rich elements (AREs) in stabilizing target gene mRNAs [29]. We performed RIP assays and observed that PABPC1 significantly binds to the 3'-UTR of WNT7A mRNA (Fig. 5W). Using AREsite2 and catRAPID, we predicted two potential PABPC1 binding sequences on the 3'-UTR of WNT7A mRNA with high ARE abundance, identified as 1,624–1,650 nt (S1) and 3,280–3,311 nt (S2) (Fig. S6 R) [24, 30]. RIP assays showed that mutation of the S1 sequence significantly impaired the interaction between PABPC1 and the 3'-UTR of WNT7A mRNA, while mutation of the S2 sequence had no effect (Fig. 5X and Fig. S6 S). Actinomycin D assays further demonstrated that mutation of the S1 segment on the 3'-UTR of WNT7A mRNA abolished PABPC1's ability to extend the half-life of WNT7A mRNA (Fig. 5Y, 5 and Fig. S6 T, U).

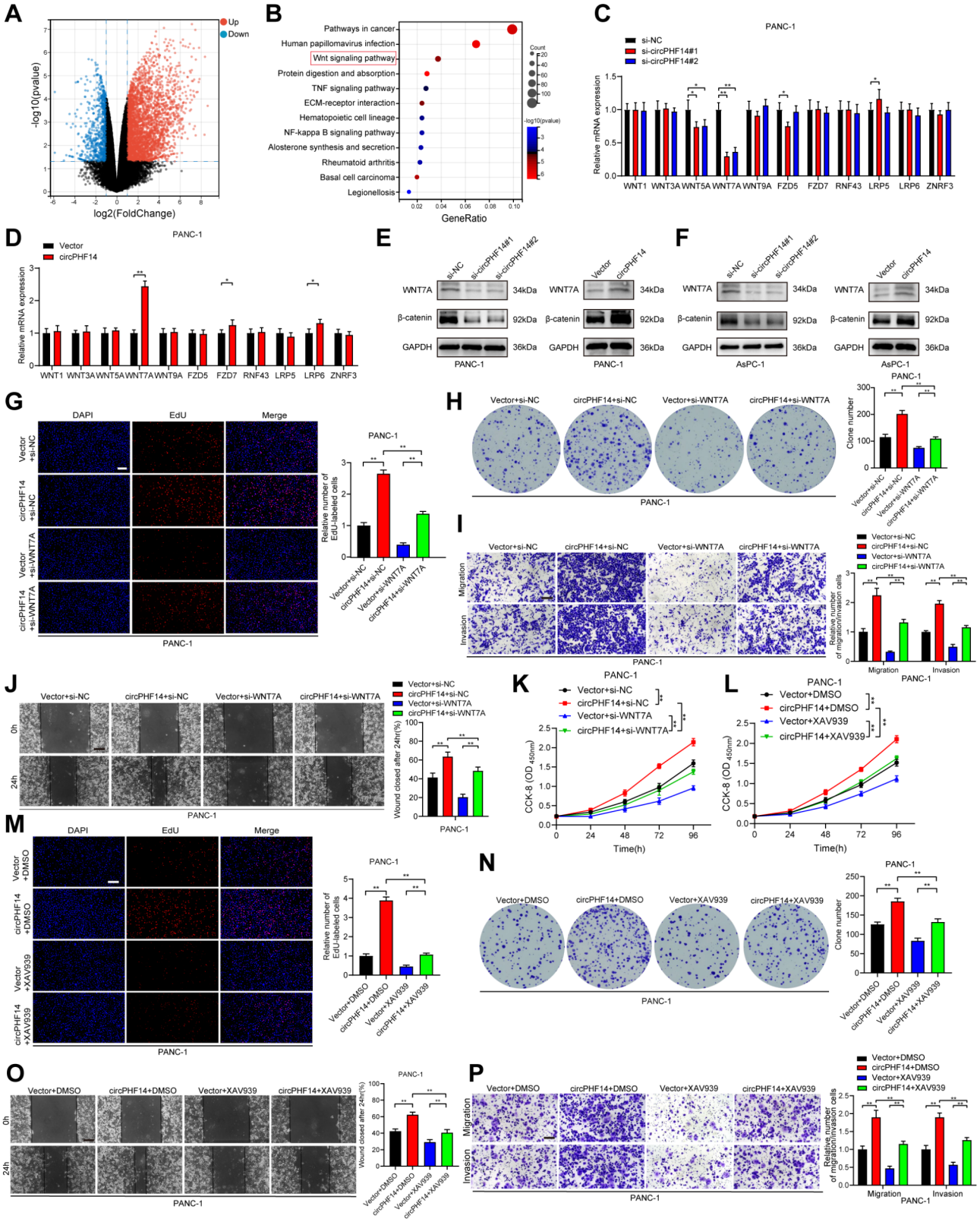

Fig. 4 (See legend on next page.)

(See figure on previous page.)

Fig. 4 CircPHF14 regulates the activation of the Wnt/β-catenin signaling pathway in PDAC. (**A**) Volcano plot of differentially expressed genes between the circPHF14 overexpression group and the control group. (**B**) KEGG pathway analysis of differentially expressed genes between the circPHF14 overexpression group and the control group. (**C, D**) qRT-PCR analysis of Wnt signaling pathway-related genes in PDAC cells with circPHF14 knockdown (**C**) or overexpression (**D**). (**E, F**) Western blot analysis of WNT7A and β-catenin expression levels in PDAC cells after circPHF14 knockdown (**E**) or overexpression (**F**). (**G**) EdU assay showing the proliferation of specified PANC-1 cells. Scale bar = 50 μm. (**H**) Representative images and statistical analysis of colony formation assays for specified PANC-1 cells. (**I**) Representative images and quantification of Transwell migration and Matrigel invasion assays for specified PANC-1 cells, Scale bar = 100 μm. (**J**) Representative images and statistical analysis of wound healing assays for specified PANC-1 cells, Scale bar = 100 μm. (**K, L**) CCK-8 assays for specified PANC-1 cells. (**M**) EdU assay showing the proliferation of specified PANC-1 cells. Scale bar = 50 μm. (**N**) Representative images and statistical analysis of colony formation assays for specified PANC-1 cells. (**O**) Representative images and statistical analysis of wound healing assays for specified PANC-1 cells, Scale bar = 100 μm. (**P**) Representative images and quantification of Transwell migration and Matrigel invasion assays for specified PANC-1 cells. Scale bar = 100 μm. Statistical differences in C, G, H, I, J, K, L, M, N, O, and P were analyzed using one-way ANOVA with Dunnett's test, and D was analyzed using a two-tailed Student's t-test. Error bars represent the standard deviation from three independent experiments. *p < 0.05, **p < 0.01

Collectively, these findings indicate that circPHF14 enhances the stability of WNT7A mRNA by binding to the 1,624–1,650 nt region of the 3'-UTR of WNT7A mRNA through PABPC1.

CircPHF14 promotes EMT by activating the Wnt pathway in PDAC

Previous studies have reported a correlation between the Wnt signaling pathway and EMT, as well as poor prognosis in PDAC [31, 32]. Therefore, we examined the expression of EMT-related genes in PDAC cells using qRT-PCR. The results showed that circPHF14 knockdown led to a downregulation of SNAI2, whereas overexpression of circPHF14 resulted in an upregulation of SNAI2 (Fig. 6A, 6). These findings were further confirmed by Western blot analysis (Fig. 6C, 6 and Fig. S7 A, B). Notably, when the Wnt pathway inhibitor XAV939 was applied to PDAC cells, qRT-PCR and Western blot analyses revealed that the upregulation of SNAI2 induced by circPHF14 overexpression was reversed (Fig. 6E, 6 and Fig. S7 C, D).

Additionally, Western blot and immunofluorescence (IF) analyses confirmed that circPHF14 knockdown increased the expression of the epithelial marker E-cadherin and inhibited the expression of the mesenchymal marker N-cadherin (Fig. 6G, 6 and Fig. S7 E, H). Conversely, circPHF14 overexpression exhibited the opposite effect (Fig. 6H, 6 and Fig. S7 F, I). Furthermore, XAV939 treatment reversed the circPHF14-mediated downregulation of E-cadherin and upregulation of N-cadherin in PDAC cells (Fig. 6I, 6 and Fig. S7 G, J). These results suggest that circPHF14 promotes EMT in PDAC through the Wnt signaling pathway.

Functionally, transwell and wound healing assays demonstrated that SNAI2 knockdown reversed the pro-migration and pro-invasion effects induced by circPHF14 overexpression in PDAC cells (Fig. 6M, 6 and Fig. S7 K, L). In conclusion, these findings indicate that circPHF14 induces EMT in PDAC by upregulating SNAI2 expression through activation of the Wnt signaling pathway.

EIF4E binds to the flanking introns of circPHF14 splicing exons to accelerate circPHF14 biogenesis in PDAC

To elucidate the molecular mechanism underlying circPHF14 upregulation in PDAC, we first used CircInteractome to predict potential RBPs interacting with circPHF14 [33]. The results suggested that EIF4A3 could bind to circPHF14; however, EIF4A3 depletion did not affect circPHF14 expression in PANC-1 cells (Fig. S8 A).

Given previous findings that 103 RBPs influence circRNA biogenesis [34]. Given the upregulation of circPHF14 in PDAC, it is likely that the RBPs promoting its biogenesis are also upregulated in this context. To investigate this, we analyzed the expression levels of these RBPs in PDAC tissues using data from The Cancer Genome Atlas (TCGA) database. Our analysis identified four RBPs that were significantly upregulated in PDAC (logFC ≥ 2, q-value < 0.01) (Fig. 7A). Next, we knocked down these four RBPs in PANC-1 cells and found that only EIF4E affected circPHF14 expression (Fig. 7B).

We further investigated the mechanism by which EIF4E regulates circPHF14 expression. It is well known that circRNA biogenesis arises from back-splicing of pre-mRNA [35]. Thus, we explored whether EIF4E promotes circPHF14 biogenesis by regulating PHF14 pre-mRNA splicing. qRT-PCR analysis showed that in PDAC cells, EIF4E knockdown or overexpression reduced or increased circPHF14 levels, respectively, without affecting PHF14 pre-mRNA expression (Fig. S8 B-E). Additionally, in PANC-1 cells, EIF4E knockdown or overexpression decreased or increased the ratio of circPHF14 to PHF14 mRNA, respectively (Fig. 7C, 7). These results suggest that EIF4E likely promotes circPHF14 biogenesis rather than enhancing the expression of the parental gene.

To confirm this, we constructed a dual color fluorescence reporter system [14, 36], which enables IRES-mediated GFP translation from circPHF14 biogenesis and mCherry expression from the linear PHF14 pre-mRNA generated by the reporter (Fig. 7E). The results showed that EIF4E knockdown in PDAC cells significantly decreased the GFP/mCherry ratio, as confirmed by Western blotting, which showed reduced GFP

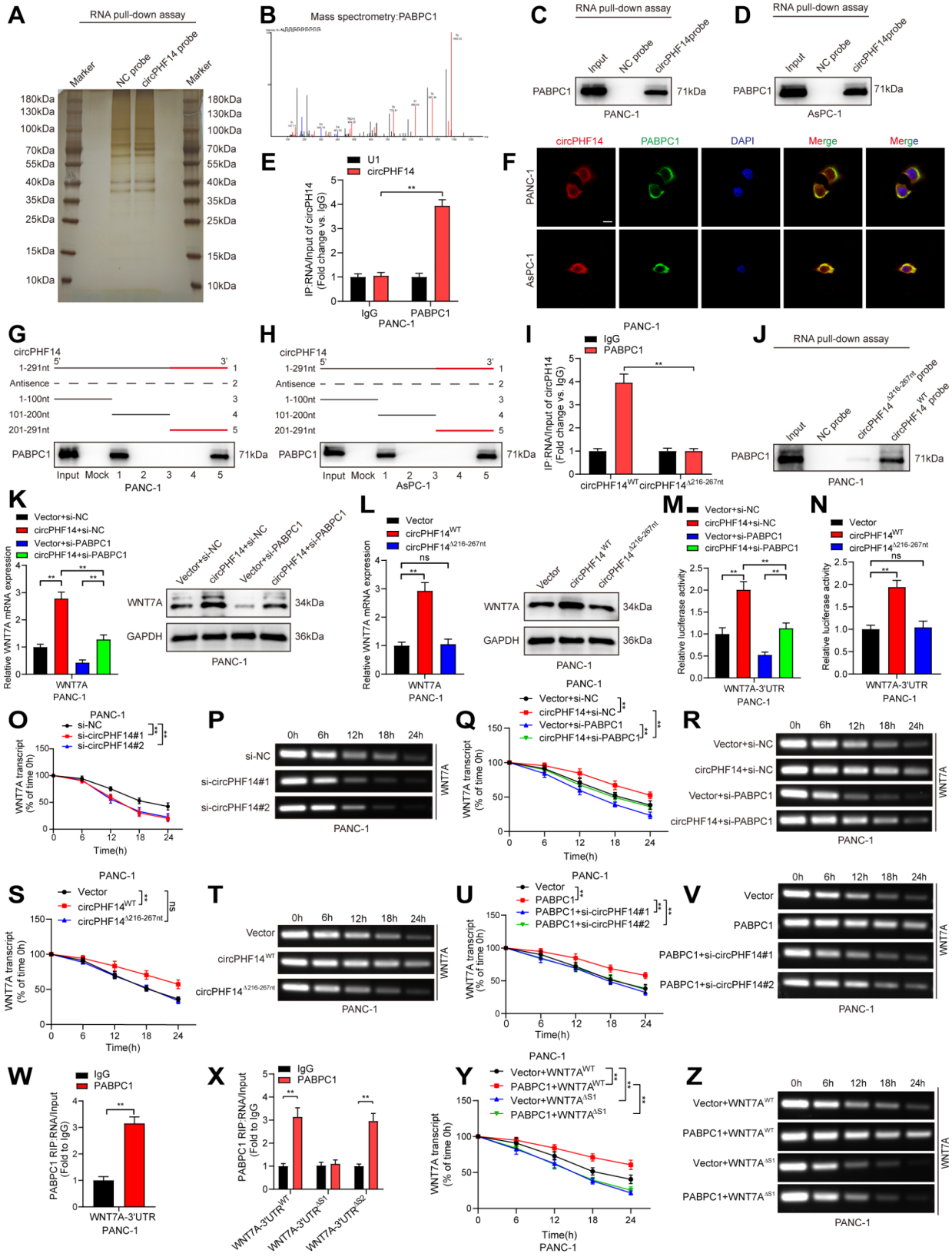

Fig. 5 (See legend on next page.)

(See figure on previous page.)

Fig. 5 CircPHF14 interacts with PABPC1 to promote WNT7A mRNA stability in PDAC cells. (**A**, **B**) Silver staining image (**A**) and mass spectrometry analysis (**B**) of PABPC1 protein identified by RNA pull-down assay using a circPHF14 probe. (**C**, **D**) Western blot analysis of the interaction between circPHF14 and PABPC1. (**E**) RIP assay confirming the enrichment of circPHF14 with PABPC1 in PANC-1 cells. (**F**) Representative images showing the colocalization of circPHF14 and PABPC1. Scale bar = 20 μm. (**G**, **H**) Sequence deletion analysis confirming that the 201–291 nt region of circPHF14 is critical for its binding to PABPC1. (**I**) RIP assay detecting the interaction after deleting the 216–267 nt region of circPHF14. (**J**) Western blot analysis of the interaction between the circPHF14 mutant and PABPC1 in PANC-1 cells. (**K**, **L**) qRT-PCR and Western blotting analysis of WNT7A expression levels in designated PANC-1 cells. (**M**, **N**) Luciferase reporter assay analyzing the activity of the WNT7A mRNA 3′-UTR in designated PANC-1 cells. (**O**-**V**) Quantification and representative agarose gel electrophoresis images of WNT7A mRNA stability detected by actinomycin D treatment in designated PANC-1 cells. (**W**) RIP assay investigating the interaction between PABPC1 and the WNT7A mRNA 3′-UTR. (**X**) RIP assay analyzing the interaction between mutated S1 and S2 sequences of the WNT7A mRNA 3′-UTR and PABPC1. (**Y**, **Z**) Quantification and representative agarose gel electrophoresis images of WNT7A mRNA stability in designated PANC-1 cells detected by actinomycin D treatment. Statistical differences in K, L, M, N, O, Q, S, U, and Y were analyzed using one-way ANOVA with Dunnett's test, and E, I, W, and X were analyzed using a two-tailed t-test. Error bars represent the standard deviation of three independent experiments. $^{*}p < 0.05$, $^{**}p < 0.01$

expression and increased mCherry expression. EIF4E overexpression showed the opposite effect (Fig. 7F-7 and Fig. S8 F-I). These results indicate that EIF4E mediates circPHF14 biogenesis in PDAC.

Previous studies have shown that circRNA biogenesis is regulated by RBPs through direct binding to the flanking introns of splicing exons, inducing circRNA circularization [6]. To determine whether EIF4E directly binds to PHF14 pre-mRNA, we conducted RIP assays (Fig. 7J and Fig. S8 J). We then designed primers targeting the introns adjacent to the circPHF14 formation exons and found that the binding of EIF4E to these adjacent regions (introns 13 and 16) was significantly higher compared to other distant regions of PHF14 pre-mRNA (Fig. 7K). To identify the exact binding sites of EIF4E on PHF14 pre-mRNA, we performed pull-down assays with truncated sequences of introns 13 and 16. Western blot analysis showed that intron 13 (100–200 nt) and intron 16 (32,500 – 33,000 nt) were particularly enriched with EIF4E (Fig. 7L, 7 and Fig. S8 K, L). Using catRAPID, we further predicted the specific binding sites of EIF4E on PHF14 pre-mRNA. The results showed that mutations in intron 13 (125–176 nt) and intron 16 (32,726 – 32,777 nt) disrupted EIF4E binding to PHF14 pre-mRNA, indicating that EIF4E directly binds to these regions (Fig. 7N-7 and Fig. S8 M, N). Additionally, complementary sequences for EIF4E binding were found near intron 13 (125–176 nt) and intron 16 (32,726 – 32,777 nt) (Fig. 7R).

To assess whether the interaction between EIF4E and PHF14 pre-mRNA affects circPHF14 production in PDAC, we performed CRISPR/Cas9-mediated deletions of intron 13 (125–176 nt) and intron 16 (32,726 – 32,777 nt) in PHF14 pre-mRNA. These deletions significantly reduced the EIF4E-mediated upregulation of circPHF14 (Fig. 7S and Fig. S8 O-Q).

In conclusion, our results indicate that EIF4E promotes circPHF14 biogenesis in PDAC by binding to specific regions of PHF14 pre-mRNA (intron 13 [125–176 nt] and intron 16 [32,726 – 32,777 nt]).

LNP-encapsulated sh-circPHF14 plasmid reveals a new therapeutic strategy for PDAC

The LNP delivery strategy represents a revolutionary advancement in therapeutics, effectively protecting and delivering a range of therapeutic molecules, including siRNA, mRNA, DNA, and small-molecule drugs. This approach ensures that these molecules are shielded from degradation and precisely delivered to target cells or tissues [37]. To explore the therapeutic potential of LNP delivery in PDAC, we encapsulated sh-circPHF14 plasmid and its control sh-NC plasmid into LNPs using liposome and microfluidic technologies (Fig. 8A). Electron microscopy revealed the structural characteristics of the LNPs (Fig. 8B). Dynamic light scattering (DLS) results indicated that the average diameters of LNP-sh-NC and LNP-sh-circPHF14 were 182.9 nm and 186.8 nm, respectively (Fig. 8C). Agarose gel electrophoresis confirmed that LNP-sh-NC and LNP-sh-circPHF14 exhibited no electrophoretic shifts compared to free plasmid, suggesting successful encapsulation of sh-NC and sh-circPHF14 plasmids into LNPs (Fig. 8D).

To further evaluate the antitumor effects of LNP-sh-circPHF14, we established a PDX model using PDAC tissues to assess the therapeutic efficacy of LNP-sh-circPHF14 (Fig. 8E). When PDX tumors reached 150 mm^3, NSG mice were randomly assigned to two groups and administered LNP-sh-NC or LNP-sh-circPHF14 via tail vein injection twice a week for five weeks. The results showed that LNP-sh-circPHF14 treatment significantly inhibited tumor growth in the PDX model compared

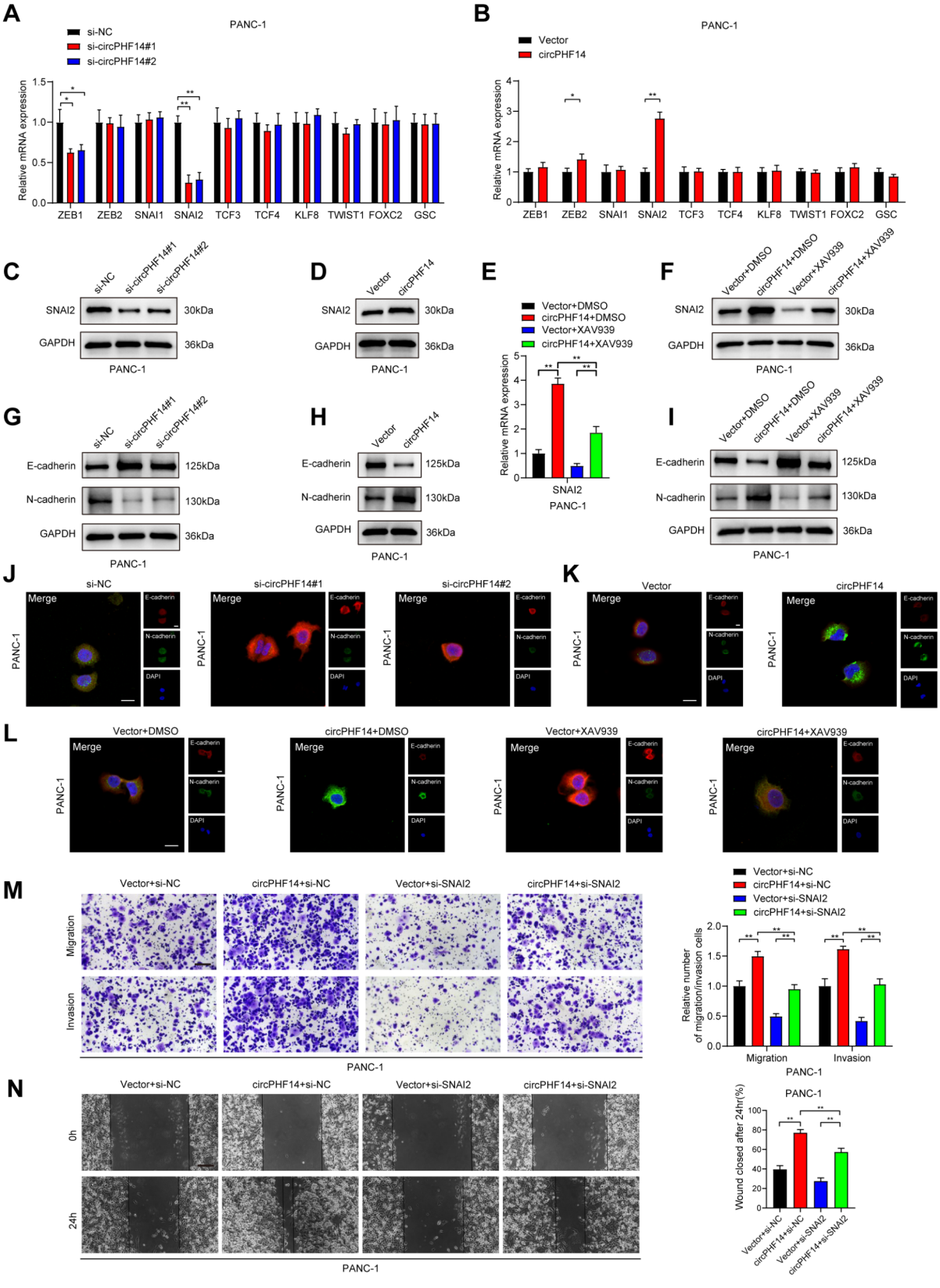

Fig. 6 (See legend on next page.)

(See figure on previous page.)

Fig. 6 CircPHF14 promotes EMT by activating the WNT7A/SNAI2 axis in PDAC. (A, B) qRT-PCR analysis of EMT-related gene expression in PANC-1 cells with circPHF14 knockdown (A) or overexpression (B). (C, D) Western blot analysis of SNAI2 expression in PANC-1 cells with circPHF14 knockdown (C) or overexpression (D). (E, F) qRT-PCR (E) and Western blot (F) analysis of SNAI2 expression in specified PANC-1 cells. (G, H) Western blot analysis of E-cadherin and N-cadherin expression in PANC-1 cells with circPHF14 knockdown (G) or overexpression (H). (I) Western blot analysis of E-cadherin and N-cadherin expression in specified PANC-1 cells. (J, K) IF analysis of E-cadherin and N-cadherin expression in PANC-1 cells with low (J) and high (K) circPHF14 expression, scale bar = 20 μm. (L) IF analysis of E-cadherin and N-cadherin expression in specified PANC-1 cells, scale bar = 20 μm. (M) Representative images and quantification of Transwell migration and Matrigel invasion assays in specified PANC-1 cells, scale bar = 100 μm. (N) Representative images and quantification of wound healing assays in specified PANC-1 cells, scale bar = 100 μm. Statistical differences in A, E, M, and N were assessed using one-way ANOVA with Dunnett's test, while two-tailed t-tests were used in B. Error bars represent the standard deviation of three independent experiments. $^{*}p < 0.05$, $^{**}p < 0.01$

to the control group (Fig. 8F). Additionally, analysis of downstream molecules in PDX tumors revealed that silencing circPHF14 significantly reduced the expression of WNT7A, β-catenin, and SNAI2 compared to the control group (Fig. 8G).

These findings demonstrate that LNP-sh-circPHF14 effectively suppresses PDAC progression and suggest that the use of LNP-encapsulated sh-circPHF14 plasmid offers a promising and safe therapeutic strategy for PDAC.

Discussion

Despite recent advances in research and treatment, the prognosis for PDAC remains poor. The absence of specific biomarkers and effective therapies is widely considered the primary cause of the poor prognosis in PDAC patients [4]. Advances in RNA sequencing technology have led to the identification of numerous circRNAs that play significant roles in tumorigenesis, disproving their previous classification as transcriptional "noise" [6]. CircRNAs, which are covalently closed circular structures with greater stability than traditional mRNAs, have garnered considerable attention from cancer researchers. CircRNAs are increasingly regarded as potential tumor biomarkers or therapeutic targets [38, 39]. Thus, investigating key circRNAs that drive PDAC proliferation and metastasis, along with their molecular mechanisms, is crucial for advancing PDAC diagnosis and treatment.

Our study identified that circPHF14 is highly expressed in PDAC and correlates with poor patient prognosis. In vivo and in vitro experiments confirmed that circPHF14 promotes PDAC cell growth and metastasis. Transcriptome sequencing revealed that overexpression of circPHF14 in PDAC cells significantly activated the canonical Wnt signaling pathway compared to controls. The Wnt pathway is crucial for regulating cancer progression, cell migration, and proliferation in multiple cancers [16, 40]. However, the mechanism by which Wnt signaling is activated in PDAC remains unclear. Our study is the first to report that circPHF14 activates the Wnt signaling pathway by stabilizing WNT7A mRNA, which in turn upregulates SNAI2, promoting EMT in PDAC. SNAI2 directly suppresses epithelial markers and activates mesenchymal markers. This disruption of cell adhesion facilitates the transition from an epithelial to a mesenchymal phenotype, leading to loss of polarity and adhesion, and enhancing cell migration and invasion [18, 20].

Our findings highlight the importance of WNT7A and SNAI2 in PDAC progression. Both may serve as promising therapeutic targets, warranting further investigation. Inhibition of the Wnt signaling pathway with the XAV939 inhibitor partially mitigated the pro-tumor effects of circPHF14 in PDAC cells in vitro. However, the promotive role of Wnt signaling in PDAC has not been extensively validated in vivo. Further studies are required to clarify the clinical relevance of the WNT7A/SNAI2 axis in PDAC.

CircRNAs have diverse biological functions, with earlier research primarily highlighting their role as miRNA sponges in regulating cellular functions. Recently, researchers have discovered that circRNAs can interact with proteins [7]. Through protein interactions, circRNAs can either sequester or activate proteins, thereby regulating cellular signaling pathways, among other functions [41]. In this study, RNA pull-down assays and mass spectrometry confirmed the interaction between circPHF14 and PABPC1. PABPC1, part of the PABP family, plays

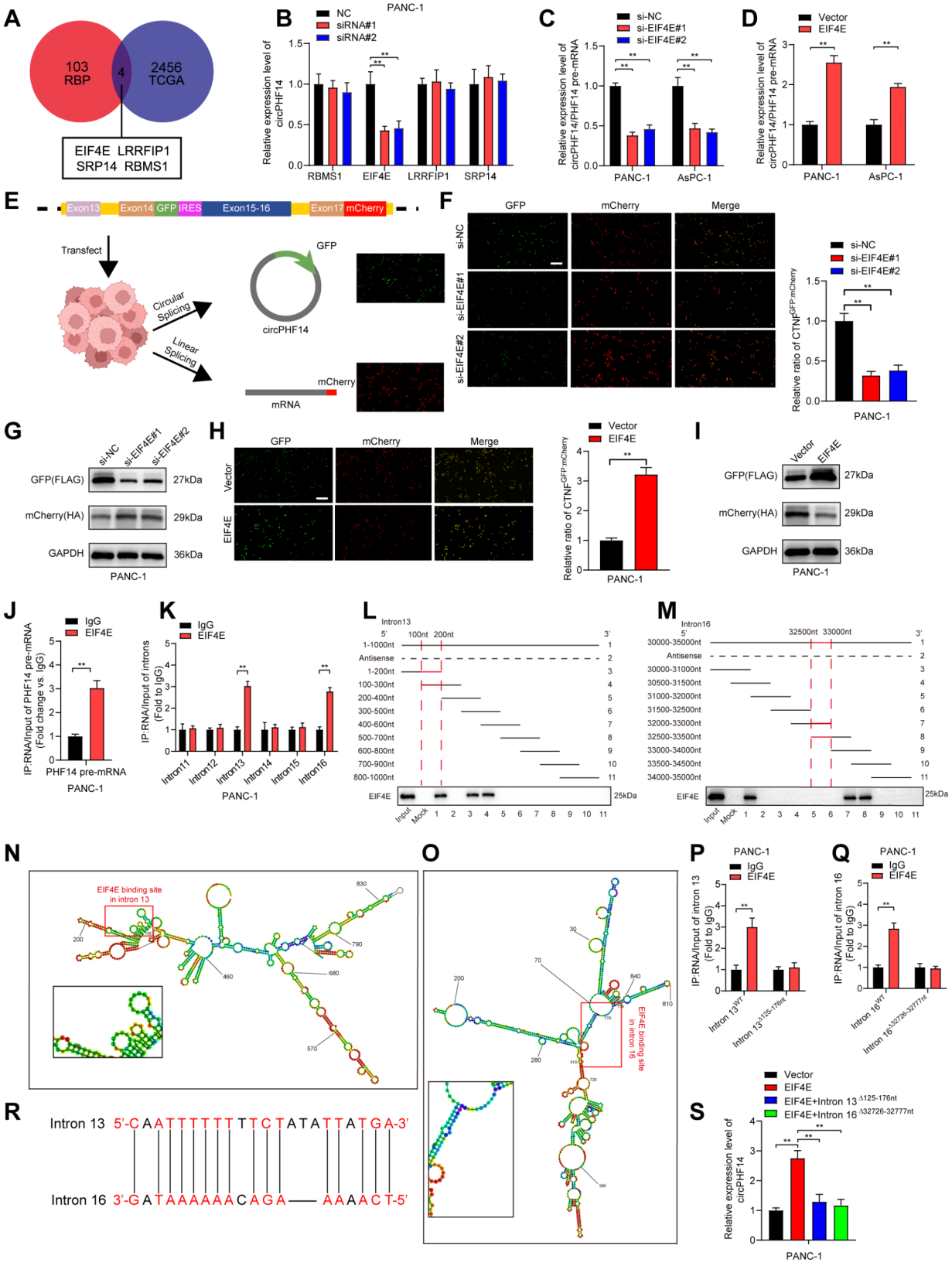

Fig. 7 (See legend on next page.)

(See figure on previous page.)

Fig. 7 EIF4E binds to flanking introns of circPHF14 splicing exons to accelerate circPHF14 biogenesis in PDAC. (**A**) Schematic diagram screening four RBPs potentially affecting circRNA production in PDAC. (**B**) qRT-PCR analysis of circPHF14 expression after knockdown of RBMS1, EIF4E, LRRFIP1, and SRP14. (**C**, **D**) Relative expression of the circPHF14/PHF14 pre-mRNA ratio after EIF4E knockdown (**C**) or overexpression (**D**). (**E**) Schematic diagram of dual color fluorescence reporter (**F**) Representative images and quantification of circPHF14 and PHF14 mRNA expression in EIF4E knockdown PANC-1 cells, scale bar = 50 μm. (**G**) Western blotting analysis of GFP and mCherry expression in EIF4E knockdown PANC-1 cells. (**H**) Representative images and quantification of circPHF14 and PHF14 mRNA expression in EIF4E overexpression PANC-1 cells, scale bar = 50 μm. (**I**) Western blotting analysis of GFP and mCherry expression in EIF4E overexpression PANC-1 cells. (**J**) RIP assay exploring the interaction between EIF4E and PHF14 pre-mRNA in PANC-1 cells. (**K**) RIP assay exploring the interaction between EIF4E and introns 11–16. (**L**, **M**) RNA pull-down assays using truncated sequences of intron 13 (**L**) and intron 16 (**M**) to identify regions necessary for interaction with EIF4E. (**N, O**) Schematic diagrams predicting binding sites of EIF4E on intron 13 (**N**) and intron 16 (**O**). (**P**, **Q**) RIP assays exploring the interaction between EIF4E and intron 13 (125-176nt) (**P**) and intron 16 (32,726-32,777nt) (**Q**) after point mutations. (**R**) Schematic diagram of complementary reverse sequences in introns 13 and 16. (**S**) Expression of circPHF14 in PANC-1 cells after knocking out EIF4E binding sites in introns 13 and 16. Statistical differences in B, C, F, and S were assessed using one-way ANOVA with Dunnett's test, while two-tailed Student's t-tests were used in D, H, J, K, P, and Q. Error bars represent the standard deviation of three independent experiments. *$p < 0.05$, **$p < 0.01$

critical roles in gene expression, particularly by binding to the 3'-UTR of mRNA to regulate stability [26, 42]. Our study first demonstrated that PABPC1 enhances WNT7A mRNA stability, a process mediated by circPHF14. While PABPC1 binds various RNAs and performs diverse functions, its precise regulatory mechanisms remain unclear, and further investigation is needed.

Understanding circRNA biogenesis in PDAC could enhance our knowledge of how circRNAs are specifically produced and accumulated during PDAC progression. However, research in this area remains limited. CircRNA biogenesis primarily occurs via back-splicing [43], with splicing factors such as RBPs (e.g., QKI and FUS) promoting circRNA formation by binding to pre-mRNA [14]. For instance, Jiang et al. reported that FUS enhances circRHOBTB3 production, promoting PDAC proliferation [44]. Our study is the first to experimentally confirm that EIF4E binds to the 125-176nt region of intron 13 and the 32,726-32,777nt region of intron 16 of PHF14 pre-mRNA, regulating its splicing and promoting circPHF14 biogenesis.

Although primarily known for promoting mRNA translation, EIF4E also contributes to mRNA splicing and post-transcriptional regulation [45]. Reports of EIF4E's role in regulating circRNA biogenesis are rare. Our findings open new avenues for studying EIF4E and its role in mRNA splicing. However, whether EIF4E generally promotes circRNA biogenesis in PDAC remains to be determined and requires further validation. The literature indicates that EIF4E is involved in the Wnt pathway, primarily by promoting the translation of associated mRNAs. For example, Wang et al. demonstrated that targeting and inhibiting the MNK/EIF4E axis reduces nuclear β-catenin levels, thereby suppressing the Wnt signaling pathway and ultimately inhibiting the proliferation, invasion, and metastasis of nasopharyngeal carcinoma [46]. Similarly, research by Patil et al. revealed that phosphorylation of EIF4E at Ser209 specifically enhances the translation of components within the Wnt signaling pathway, playing a critical role in sustaining synaptic activity-induced long-term potentiation [47]. Furthermore, this study confirmed that EIF4E accelerates the biogenesis of circPHF14, which subsequently activates the downstream Wnt pathway. These findings provide a novel perspective on the mechanisms through which EIF4E regulates the Wnt pathway.

Although circRNAs hold great promise for cancer therapy, effectively targeting circRNAs at tumor sites remains a major challenge. LNPs can encapsulate nucleic acids (e.g., siRNA, mRNA, shRNA, circRNA) or small molecule drugs, enabling targeted cancer therapy [48]. Some researchers suggest that this challenge can be effectively addressed. For instance, Li et al. developed LNPs encapsulating plasmids carrying circUGP2, successfully targeting intrahepatic cholangiocarcinoma in mice and confirming its anti-tumor effects [49]. This LNP strategy shows considerable potential for clinical applications but also presents specific challenges.

Building on this approach, we developed LNPs encapsulating sh-circPHF14 plasmids and validated their anti-tumor efficacy in a PDX model. However, achieving efficient targeted delivery of LNPs continues to be a significant challenge. Our next step is to optimize LNPs by modifying their surface with ligands to enhance their targeting specificity in tumor models [50]. Further validation of LNP-sh-circPHF14's efficacy in treating PDAC is necessary. Consequently, we should validate its effectiveness in additional xenograft models to establish a safe and effective anti-tumor strategy for PDAC.

In conclusion, our study advances the understanding of PDAC tumorigenesis and progression and may offer novel therapeutic targets and strategies for PDAC patients.

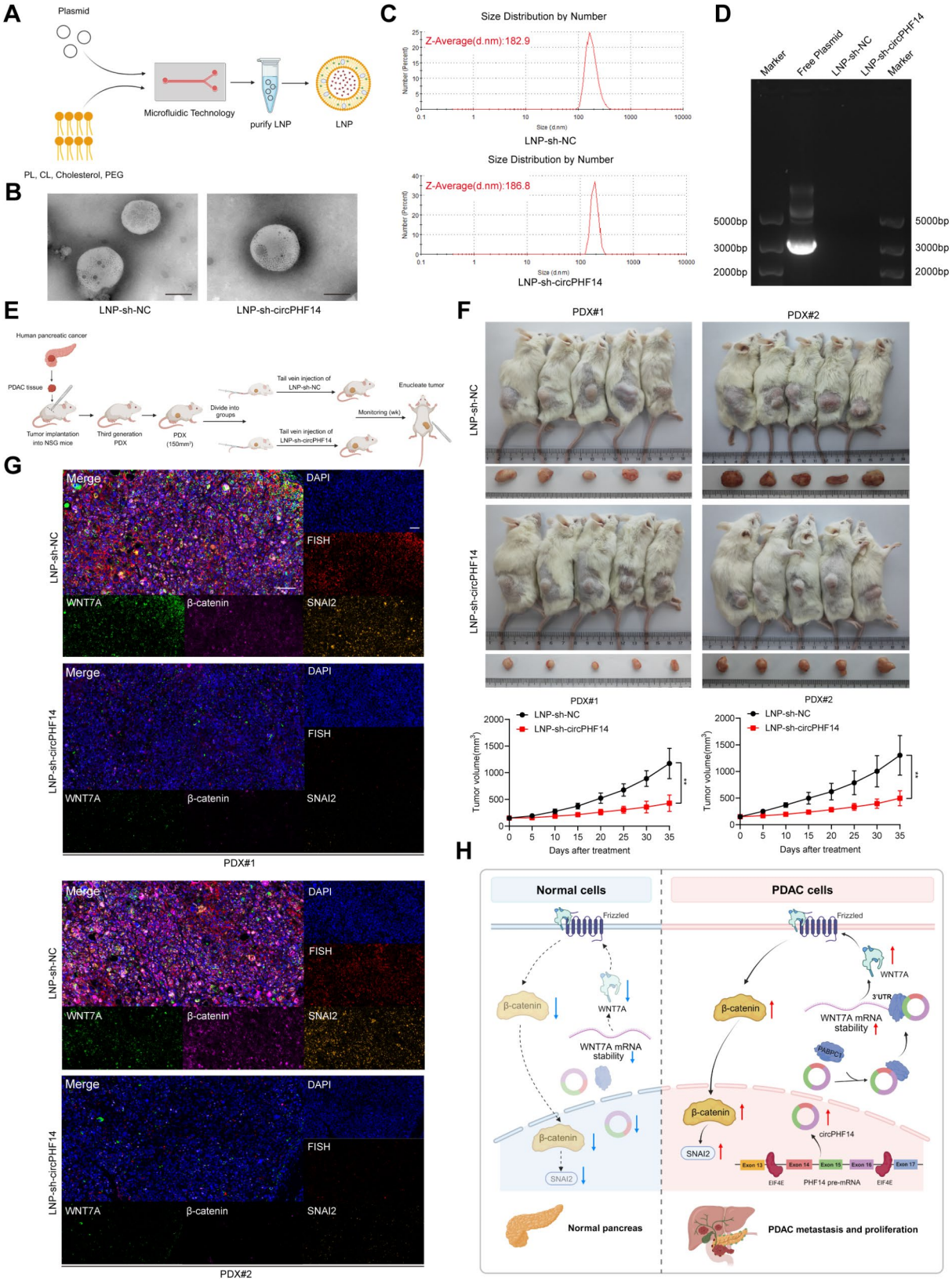

Fig. 8 (See legend on next page.)

(See figure on previous page.)

Fig. 8 Therapeutic strategy of LNP-encapsulated sh-circPHF14 plasmid reveals anti-PDAC effects. (**A**) Schematic diagram of the LNP system encapsulating sh-circPHF14 plasmid. (**B**) Representative TEM images of LNP-sh-NC and LNP-sh-circPHF14 (scale bar = 100 nm). (**C**) Diameter measurement of LNP-sh-NC and LNP-sh-circPHF14 using DLS. (**D**) Agarose gel electrophoresis analysis of free plasmid, LNP-sh-NC, and LNP-sh-circPHF14. (**E**) Schematic diagram of PDX model construction. (**F**) Images and quantification of tumor volumes in mice treated with LNP-sh-NC or LNP-sh-circPHF14 ($p < 0.05$). (**G**) Representative images of multiplex immunohistochemical staining for WNT7A, β-catenin, and SNAI2 expression. Scale bar = 100 μm. (**H**) Scientific schematic diagram. Statistical significance in F was assessed using two-tailed Student's t-test. Error bars represent the standard deviation of three independent experiments. *$p < 0.05$, **$p < 0.01$

Conclusions

In conclusion, our study reveals that circPHF14 is markedly upregulated in both PDAC cells and clinical samples. Mechanistically, we identified that EIF4E-mediated circPHF14 stabilizes WNT7A mRNA through its interaction with PABPC1, leading to the activation of the Wnt/β-catenin pathway in PDAC. Furthermore, circPHF14 upregulates SNAI2 expression via the Wnt/β-catenin pathway, which significantly enhances PDAC proliferation and metastasis. These findings suggest that circPHF14 may serve as a promising diagnostic biomarker and therapeutic target for PDAC.

Abbreviations

AREs	(AU)-rich elements
BCA	Bicinchoninic acid
CCK-8	Cell counting kit-8
cDNA	Complementary DNA
circRNA	Circular RNA
DAPI	4′,6-Diamidino-2-phenylindole
DLS	Dynamic light scattering
DMEM	Dulbecco's modified eagle medium
EdU	5-Ethynyl-2′-deoxyuridine
EMT	Epithelial-mesenchymal transition
FBS	Fetal bovine serum
FISH	Fluorescence in situ hybridization
gDNA	Genomic DNA
HE	Hematoxylin and eosin
IF	Immunofluorescence
IHC	Immunohistochemistry
IVIS	In vivo imaging system
KEGG	Kyoto encyclopedia of genes and genomes
LNP	Lipid Nanoparticle
NC	Negative control
OS	Overall survival
PBS	Phosphate-buffered saline
PDAC	Pancreatic ductal adenocarcinoma
PDX	Patient-derived Xenograft
QRT-PCR	Quantitative real-time polymerase chain reaction
RBPs	RNA-binding proteins
RIP	RNA Immunoprecipitation
RIPA	Radioimmunoprecipitation assay
SiRNAs	Small interfering RNAs
TBST	Tris-Buffered saline with Tween-20
TCGA	The cancer genome atla
3′-UTR	3′ untranslated region

Supplementary Information

The online version contains supplementary material available at https://doi.org/10.1186/s12943-025-02262-5.

Supplementary Material 1

Acknowledgements

We thank all the patients and their families for their participation.

Author contributions

Z.F., Z.W. and R.C. conceived and designed the experiments. Z.F., Z.W., C.Y. and Q.X. performed most of the experiments and data analysis. Z.F. drafted the manuscript. C.Y., Q.X., and L.Z. performed the bioinformatic analysis and revised the work critically for important intellectual content. Z.F. and Z.W. performed the in vitro and in vivo experiments and data analyses. C.Y. and Q.X. helped with the in vivo experiments. L.Z. collected the clinical samples and information. All authors read and approved the final manuscript.

Funding

This study was funded by the "Dengfeng Plan" Special Fund of Guangdong Provincial People's Hospital (KJ012019509, DFJH2020027); National Natural Science Foundation of China (KB012023494, 2372858, KY012023604, 2372858); the Guangzhou Key Research and Development Supplementary Support Program (KE012024221, 2024B01J13795).

Data availability

Data is provided within the manuscript or supplementary information files.

Declarations

Ethics approval and consent to participate

All clinical data and specimens involved in this study were obtained with written informed consent from the patients and approved by the Ethics Committee of Guangdong Provincial People's Hospital. All animal experiments were conducted in accordance with the regulations of the Ethics Committee of Guangdong Provincial People's Hospital.

Consent for publication

All authors have provided written informed consent and have agreed to the uniform publication of this manuscript.

Competing interests

The authors declare no competing interests.

Received: 24 October 2024 / Accepted: 6 February 2025
Published online: 26 February 2025

References

1. Ryan DP, Hong TS, Bardeesy N. Pancreatic adenocarcinoma. N Engl J Med. 2014;371:1039–49.
2. Siegel RL, Giaquinto AN, Jemal A. Cancer statistics, 2024. CA Cancer J Clin. 2024;74:12–49.
3. Neoptolemos JP, Kleeff J, Michl P, Costello E, Greenhalf W, Palmer DH. Therapeutic developments in pancreatic cancer: current and future perspectives. Nat Rev Gastroenterol Hepatol. 2018;15:333–48.
4. Kleeff J, Korc M, Apte M, La Vecchia C, Johnson CD, Biankin AV, Neale RE, Tempero M, Tuveson DA, Hruban RH, Neoptolemos JP. Pancreatic cancer. Nat Rev Dis Primers. 2016;2:16022.
5. Conroy T, Hammel P, Hebbar M, Ben Abdelghani M, Wei AC, Raoul JL, Choné L, Francois E, Artru P, Biagi JJ, et al. FOLFIRINOX or Gemcitabine as Adjuvant Therapy for Pancreatic Cancer. N Engl J Med. 2018;379:2395–406.
6. Kristensen LS, Andersen MS, Stagsted LVW, Ebbesen KK, Hansen TB, Kjems J. The biogenesis, biology and characterization of circular RNAs. Nat Rev Genet. 2019;20:675–91.
7. Patop IL, Wüst S, Kadener S. Past, present, and future of circRNAs. Embo j. 2019;38:e100836.
8. Yang R, Cui J. Advances and applications of RNA vaccines in tumor treatment. Mol Cancer. 2024;23:226.

9. Rong Z, Xu J, Shi S, Tan Z, Meng Q, Hua J, Liu J, Zhang B, Wang W, Yu X, Liang C. Circular RNA in pancreatic cancer: a novel avenue for the roles of diagnosis and treatment. Theranostics. 2021;11:2755–69.
10. Guo X, Zhou Q, Su D, Luo Y, Fu Z, Huang L, Li Z, Jiang D, Kong Y, Li Z, et al. Circular RNA circBFAR promotes the progression of pancreatic ductal adenocarcinoma via the miR-34b-5p/MET/Akt axis. Mol Cancer. 2020;19:83.
11. Xiao MS, Ai Y, Wilusz JE. Biogenesis and functions of circular RNAs come into Focus. Trends Cell Biol. 2020;30:226–40.
12. Li Y, Kong Y, An M, Luo Y, Zheng H, Lin Y, Chen J, Yang J, Liu L, Luo B, et al. ZEB1-mediated biogenesis of circNIPBL sustains the metastasis of bladder cancer via Wnt/β-catenin pathway. J Exp Clin Cancer Res. 2023;42:191.
13. Ashwal-Fluss R, Meyer M, Pamudurti NR, Ivanov A, Bartok O, Hanan M, Evantal N, Memczak S, Rajewsky N, Kadener S. circRNA biogenesis competes with pre-mRNA splicing. Mol Cell. 2014;56:55–66.
14. Conn SJ, Pillman KA, Toubia J, Conn VM, Salmanidis M, Phillips CA, Roslan S, Schreiber AW, Gregory PA, Goodall GJ. The RNA binding protein quaking regulates formation of circRNAs. Cell. 2015;160:1125–34.
15. Errichelli L, Dini Modigliani S, Laneve P, Colantoni A, Legnini I, Capauto D, Rosa A, De Santis R, Scarfò R, Peruzzi G, et al. FUS affects circular RNA expression in murine embryonic stem cell-derived motor neurons. Nat Commun. 2017;8:14741.
16. Anastas JN, Moon RT. WNT signalling pathways as therapeutic targets in cancer. Nat Rev Cancer. 2013;13:11–26.
17. Chien AJ, Conrad WH, Moon RT. A wnt survival guide: from flies to human disease. J Invest Dermatol. 2009;129:1614–27.
18. Lamouille S, Xu J, Derynck R. Molecular mechanisms of epithelial-mesenchymal transition. Nat Rev Mol Cell Biol. 2014;15:178–96.
19. Kalluri R, Weinberg RA. The basics of epithelial-mesenchymal transition. J Clin Invest. 2009;119:1420–8.
20. Peinado H, Olmeda D, Cano A. Snail, Zeb and bHLH factors in tumour progression: an alliance against the epithelial phenotype? Nat Rev Cancer. 2007;7:415–28.
21. Yoshioka S, King ML, Ran S, Okuda H, MacLean JA 2nd, McAsey ME, Sugino N, Brard L, Watabe K, Hayashi K. WNT7A regulates tumor growth and progression in ovarian cancer through the WNT/β-catenin pathway. Mol Cancer Res. 2012;10:469–82.
22. Shi J, Kantoff PW, Wooster R, Farokhzad OC. Cancer nanomedicine: progress, challenges and opportunities. Nat Rev Cancer. 2017;17:20–37.
23. Cullis PR, Hope MJ. Lipid nanoparticle systems for enabling Gene therapies. Mol Ther. 2017;25:1467–75.
24. Agostini F, Zanzoni A, Klus P, Marchese D, Cirillo D, Tartaglia GG. catRAPID omics: a web server for large-scale prediction of protein-RNA interactions. Bioinformatics. 2013;29:2928–30.
25. Li B, Zhu L, Lu C, Wang C, Wang H, Jin H, Ma X, Cheng Z, Yu C, Wang S, et al. circNDUFB2 inhibits non-small cell lung cancer progression via destabilizing IGF2BPs and activating anti-tumor immunity. Nat Commun. 2021;12:295.
26. Fatscher T, Boehm V, Weiche B, Gehring NH. The interaction of cytoplasmic poly(A)-binding protein with eukaryotic initiation factor 4G suppresses nonsense-mediated mRNA decay. RNA. 2014;20:1579–92.
27. Wei W, Liu K, Huang X, Tian S, Wang H, Zhang C, Ye J, Dong Y, An Z, Ma X, et al. EIF4A3-mediated biogenesis of circSTX6 promotes bladder cancer metastasis and cisplatin resistance. J Exp Clin Cancer Res. 2024;43:2.
28. Muppirala UK, Honavar VG, Dobbs D. Predicting RNA-protein interactions using only sequence information. BMC Bioinformatics. 2011;12:489.
29. Nabors LB, Gillespie GY, Harkins L, King PH. HuR, a RNA stability factor, is expressed in malignant brain tumors and binds to adenine- and uridine-rich elements within the 3′ untranslated regions of cytokine and angiogenic factor mRNAs. Cancer Res. 2001;61:2154–61.
30. Fallmann J, Sedlyarov V, Tanzer A, Kovarik P, Hofacker IL. AREsite2: an enhanced database for the comprehensive investigation of AU/GU/U-rich elements. Nucleic Acids Res. 2016;44:D90–95.
31. Todoric J, Karin M. The fire within: Cell-Autonomous mechanisms in inflammation-driven Cancer. Cancer Cell. 2019;35:714–20.
32. Dong D, Yu X, Xu J, Yu N, Liu Z, Sun Y. Cellular and molecular mechanisms of gastrointestinal cancer liver metastases and drug resistance. Drug Resist Updat. 2024;77:101125.
33. Dudekula DB, Panda AC, Grammatikakis I, De S, Abdelmohsen K, Gorospe M. CircInteractome: a web tool for exploring circular RNAs and their interacting proteins and microRNAs. RNA Biol. 2016;13:34–42.
34. Li X, Liu CX, Xue W, Zhang Y, Jiang S, Yin QF, Wei J, Yao RW, Yang L, Chen LL. Coordinated circRNA Biogenesis and function with NF90/NF110 in viral infection. Mol Cell. 2017;67:214–e227217.
35. Yang L, Wilusz JE, Chen LL. Biogenesis and Regulatory roles of Circular RNAs. Annu Rev Cell Dev Biol. 2022;38:263–89.
36. Kong Y, Luo Y, Zheng S, Yang J, Zhang D, Zhao Y, Zheng H, An M, Lin Y, Ai L, et al. Mutant KRAS mediates circARFGEF2 Biogenesis to promote lymphatic metastasis of pancreatic ductal adenocarcinoma. Cancer Res. 2023;83:3077–94.
37. Witzigmann D, Kulkarni JA, Leung J, Chen S, Cullis PR, van der Meel R. Lipid nanoparticle technology for therapeutic gene regulation in the liver. Adv Drug Deliv Rev. 2020;159:344–63.
38. Li X, Yang L, Chen LL. The Biogenesis, functions, and challenges of Circular RNAs. Mol Cell. 2018;71:428–42.
39. Vo JN, Cieslik M, Zhang Y, Shukla S, Xiao L, Zhang Y, Wu YM, Dhanasekaran SM, Engelke CG, Cao X, et al. The Landscape of circular RNA in Cancer. Cell. 2019;176:869–e881813.
40. von Maltzahn J, Chang NC, Bentzinger CF, Rudnicki MA. Wnt signaling in myogenesis. Trends Cell Biol. 2012;22:602–9.
41. Li Z, Huang C, Bao C, Chen L, Lin M, Wang X, Zhong G, Yu B, Hu W, Dai L, et al. Exon-intron circular RNAs regulate transcription in the nucleus. Nat Struct Mol Biol. 2015;22:256–64.
42. Lim J, Ha M, Chang H, Kwon SC, Simanshu DK, Patel DJ, Kim VN. Uridylation by TUT4 and TUT7 marks mRNA for degradation. Cell. 2014;159:1365–76.
43. Zhang XO, Wang HB, Zhang Y, Lu X, Chen LL, Yang L. Complementary sequence-mediated exon circularization. Cell. 2014;159:134–47.
44. Yang T, Shen P, Chen Q, Wu P, Yuan H, Ge W, Meng L, Huang X, Fu Y, Zhang Y, et al. FUS-induced circRHOBTB3 facilitates cell proliferation via miR-600/NACC1 mediated autophagy response in pancreatic ductal adenocarcinoma. J Exp Clin Cancer Res. 2021;40:261.
45. Ghram M, Morris G, Culjkovic-Kraljacic B, Mars JC, Gendron P, Skrabanek L, Revuelta MV, Cerchietti L, Guzman ML, Borden KLB. The eukaryotic translation initiation factor eIF4E reprograms alternative splicing. Embo j. 2023;42:e110496.
46. Wang W, Wen Q, Luo J, Chu S, Chen L, Xu L, Zang H, Alnemah MM, Li J, Zhou J, Fan S. Suppression of β-catenin nuclear translocation by CGP57380 decelerates poor progression and Potentiates Radiation-Induced apoptosis in nasopharyngeal carcinoma. Theranostics. 2017;7:2134–49.
47. Patil S, Chalkiadaki K, Mergiya TF, Krimbacher K, Amorim IS, Akerkar S, Gkogkas CG, Bramham CR. eIF4E phosphorylation recruits β-catenin to mRNA cap and promotes wnt pathway translation in dentate gyrus LTP maintenance. iScience. 2023;26:106649.
48. Hou X, Zaks T, Langer R, Dong Y. Lipid nanoparticles for mRNA delivery. Nat Rev Mater. 2021;6:1078–94.
49. Chen RX, Liu SC, Kan XC, Wang YR, Wang JF, Wang TL, Li C, Jiang WJ, Chen YAL, Zhou T, et al. CircUGP2 suppresses Intrahepatic Cholangiocarcinoma Progression via p53 signaling through interacting with PURB to regulate ADGRB1 transcription and sponging miR-3191-5p. Adv Sci (Weinh). 2024;11:e2402329.
50. Akinc A, Maier MA, Manoharan M, Fitzgerald K, Jayaraman M, Barros S, Ansell S, Du X, Hope MJ, Madden TD, et al. The Onpattro story and the clinical translation of nanomedicines containing nucleic acid-based drugs. Nat Nanotechnol. 2019;14:1084–7.

Publisher's note